

Measured gain suppression in FBK LGADs with different active thicknesses

**J. Yang¹ S. Braun⁴ Q. Buat¹ J. Ding² M. Harrison⁵ P. Kammel¹ S.M. Mazza²
F. McKinney-Martinez² A. Molnar² J. Ott³ A. Seiden² B. Schumm² Y. Zhao⁴ Y. Zhang⁶
V. Tishchenko⁶ A. Bisht⁷ M. Centis-Vignali⁷ G. Paternoster⁷ M. Boscardin⁷**

¹*Center for Nuclear Physics and Astrophysics (CENPA), University of Washington, Seattle, WA 98195, USA*

²*SCIPP, University of California Santa Cruz, 1156 High Street, Santa Cruz (CA), 950156, US*

³*Department of Electrical and Computer Engineering, University of Hawaii at Manoa, 2540 Dole Street, Honolulu HI-96822, USA*

⁴*Physics Department, Carleton University, 1125 Colonel By Drive, Ottawa, Ontario, K1S 5B6, Canada*

⁵*Department of Physics and Astronomy, University of New Mexico, 210 Yale Blvd. NE, Albuquerque, NM 87106*

⁶*Brookhaven National Laboratories, Upton (NY), U.S.*

⁷*Fondazione Bruno Kessler*

E-mail: simazza@ucsc.edu

ABSTRACT: In recent years, the gain suppression mechanism has been studied for large localized charge deposits in Low-Gain Avalanche Detectors (LGADs). LGADs are a thin silicon detector with a highly doped gain layer that provides moderate internal signal amplification. Using the CENPA Tandem accelerator at the University of Washington, the response of LGADs with different thicknesses to MeV-range energy deposits from a proton beam were studied. Three LGAD prototypes of 50 μm , 100 μm , and 150 μm were characterized. The devices' gain was determined as a function of bias voltage, incidence beam angle, and proton energy. This study was conducted in the scope of the PIONEER experiment, an experiment proposed at the Paul Scherrer Institute to perform high-precision measurements of rare pion decays. LGADs are considered for the active target (ATAR), and energy linearity is an important property for particle ID capabilities.

KEYWORDS: Ultra Fast silicon, LGAD, gain suppression, PIONEER experiment

1 Introduction

Low Gain Avalanche Detectors (LGADs) are thin silicon detectors with internal gain [1] capable of providing a time resolution as good as 17 ps [2] for minimum-ionizing particles. LGADs are the chosen technology for near-future large-scale applications like the timing layer upgrade for HL-LHC of the ATLAS [3] and CMS [4] experiments at CERN, the ePIC detector at the Electron-Ion Collider at BNL [5] and the PIONEER experiment [6]. In particular, this study was performed for the PIONEER collaboration since energy linearity is important for particle ID between positron, muon, and pion in the active target (ATAR) [6].

This study is a continuation of a previous round of measurements done in 2023 [7]; the saturation effect has also been studied by several other research groups [8, 9]. The gain saturation is triggered by the shielding of the electric field in the gain layer caused by the multiplication of the charge carriers in the bulk, and increases with the density of the deposited charge. Therefore, it depends on the total amount of initial deposited charge, the sensor gain, and the angle of incidence with respect to the charge drift direction towards the gain layer (the charge carrier drift is more distributed across the gain layer for an angled track).

2 Experimental setup

The Center for Experimental Nuclear Physics and Astrophysics (CENPA) at the University of Washington has a High Voltage Engineering Corporation Model FN tandem Van de Graaff accelerator [10] that is used to perform various accelerator-based experiments. Protons of 1.8 MeV, 3 MeV, 3.8 MeV, 4.5 MeV, 5.5 MeV, and 6.5 MeV momenta were used for this measurement campaign for devices that have an active thickness of 50 μm , 100 μm , and 150 μm . The momentum resolution of the proton beam is around 300 ppm, and the beam size is around 2 mm, which is smaller than the Rutherford back-scattering (RBS) target size and comparable with the sensor size.

The tested LGAD sensors are mounted on a fast analog single channel electronic board (around 2 GHz bandwidth) designed at SCIPP [11] with an additional external box amplifier¹, the signal is digitized by the Sompic digitizer board [12] with 11 bit, 1-10 Gs/s digitizer and a self-triggering capability. The experimental setup is the same as in the previous article [7] using the Rutherford Backscattering (RBS) technique with 0.093 nm and 0.166 nm thick gold foils. The reference data for beta particles from a ⁹⁰Sr source was taken in the SCIPP laboratories with identical sensors and readout boards; the energy of the ⁹⁰Sr electron is in the minimum ionizing particle (MIP) range. The ⁹⁰Sr system has been previously described in detail in [2]. The CENPA test beam data and the ⁹⁰Sr data were analyzed using the package described in the “Data analysis” section of the previous article [7].

3 Sensors tested

Three single pad LGADs and three PINs (identical geometry but without gain layer) from FBK (Fondazione Bruno Kessler), were tested. The devices tested had 50 μm , 100 μm , and 150 μm of active thickness. A list of the devices’ characteristics is shown in Tab. 1. The table shows

¹GALI-52+ evaluation board

the breakdown voltage corresponding to the highest possible sensor gain. The energy deposited in the PIN detector depends on different beam energies and angles. E.g., in the 50 μm detector, At 1.8 MeV of energy, the proton always stops (stopping power 120 MeV/cm²g, range in silicon around 40 μm) and deposits about 80 fC of charge; at 3 MeV, the proton initially punches through and stops for an angle of approximately 55 degrees (stopping power 84.33 MeV/cm²g, range in silicon around 90 μm), depositing around 130 fC. In the 100 μm detector, 3 MeV protons will always stop, 4.5 MeV protons will stop after 50 degrees, and 6.5 MeV protons will pass through even after 70 degrees. In the 150 μm detector, 5.5 M will stop after 50 degrees and 6.5 MeV will stop after 60 degrees. To provide a reference, the collected charge for a MIP is around 0.5 fC/1 fC/1.5 fC for the 50 μm /100 μm /150 μm active thickness of the detector tested (Fig. 1, Left); therefore, the injected charge by the proton is around 160 and 260 MIP at 1.8 MeV and 3 MeV for a 50 μm device, respectively.

Device	Producer	BV	Thickness	Gain layer	Gain range
W1 LGAD	FBK	250 V	50 μm	very shallow	10-50
W1 PIN	FBK	400 V	50 μm	no gain	1
W8 LGAD	FBK	350 V	100 μm	very shallow	5-30
W8 PIN	FBK	500 V	100 μm	no gain	1
W11 LGAD	FBK	600 V	150 μm	very shallow	5-20
W14 PIN	FBK	700 V	150 μm	no gain	1

Table 1: List of tested FBK LGADs and PIN devices. All devices have a $2.5 \times 2.5 \text{ mm}^2$ single pad geometry. W11 and W14 have the same thickness but a difference in the gain layer. Therefore, PINs (no gain layer) from these two wafers are identical.

4 ⁹⁰Sr source Results

The sensors were tested in a laboratory with a ⁹⁰Sr radioactive source in a coincidence system to ensure observation of MIP response. The setup is composed of two identical readout boards, one with the device-under-test (DUT) and one with a known trigger sensor, aligned with a ⁹⁰Sr source. A full explanation of the whole setup can be found in Ref. [2]. The collected charge vs bias voltage is shown in Fig. 1, left for PIN devices. The charge values reflect the PIN thickness at 50 μm and 150 μm (around 0.1 fC per 10 μm), but it's off for 100 μm . The specification of the sensor thickness from FBK might not be completely correct for the 100 μm device that seems to behave as being 80 μm thick. The gain (collected charge in the LGAD divided by the collected charge of a same-thickness PIN) vs bias voltage is shown in Fig. 1, Right. Measurements were made only at a 0-degree (perpendicular) incident angle.

5 Results

The behavior of the devices was probed as a function of the proton incidence angle and applied bias voltage. The PIN sensors were tested for a limited set of voltages and showed almost no variation in the total charge deposition. The gain as a function of angle for the 50 μm , 100 μm ,

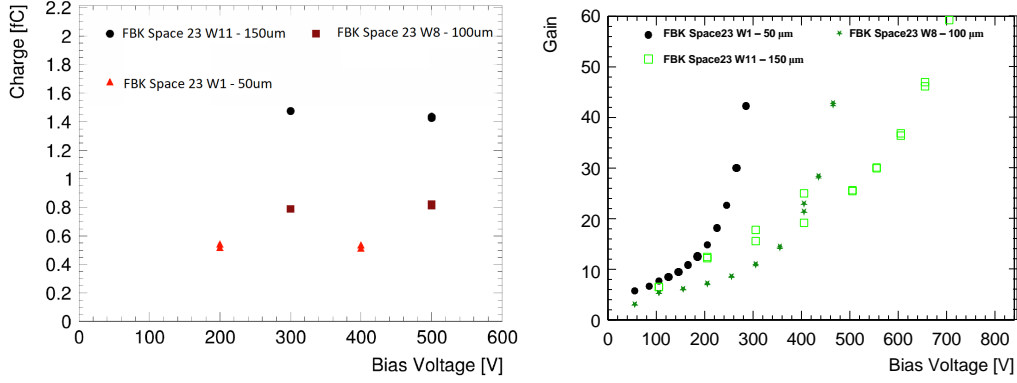


Figure 1: Left: Collected charge for Sr90 electrons as a function of bias voltage for FBK PIN detectors. Right: Gain for Sr90 electrons as a function of bias voltage for the FBK LGAD detectors. Data was taken with Sr90 source at SCIPP at 0 degrees incident angle.

and 150 μm active thickness LGAD devices for several beam energies is shown in Fig. 2 (a), (b), and (c), respectively. The gain increases with the angle of incidence up to a certain angle; then, it decreases up to the largest angle tested (75 degrees).

The electrons drifting toward the gain layer are a projection of the entry track; for a zero-degree angle, the charge density on the gain layer is highly localized, while angled tracks produce a more dispersed and, therefore, reduced charge density throughout the gain layer, so the suppression mechanism is less pronounced. The gain decrease at large angles can be explained by the competing effect of the charge deposition's proximity to the gain layer. In Ref. [13, 14], it was shown that the depth of X-ray absorption influences the sensor response such that the gain is effectively less for charge depositions closer to the gain layer. The charge lateral diffusion during drift towards the gain layer is the most likely explanation for this effect. The proton energy deposition profile has the properties of a Bragg peak, depositing a large amount of energy at the stopping point. At a large angle, the proton deposits a larger amount of charge closer to the gain layer, given that the track length is always the same when the ion stops inside the active layer.

6 Conclusions

The response to highly ionizing particles of several types of FBK LGADs and PINs was studied at the CENPA tandem accelerator with protons of several different energies. The gain in the LGADs was calculated as a function of proton energy, applied bias voltage, and angle of incidence and compared to the response of the same-size PIN detector. All LGAD devices show substantial gain suppression with respect to the gain for MIPs measured in laboratory, which is more significant for higher applied bias voltage. The suppression changes with the angle of incidence of the beam: it increases up to 40 to 60 degrees of incidence, but then it is again reduced because of the large deposition closer to the gain layer.

Comparing the results of this paper with the previous results for HPK sensors [7], the gain saturation effect is significantly more prominent, especially for the direct comparison with the 50 μm active layer device with a similar breakdown voltage. A possible explanation of the observed

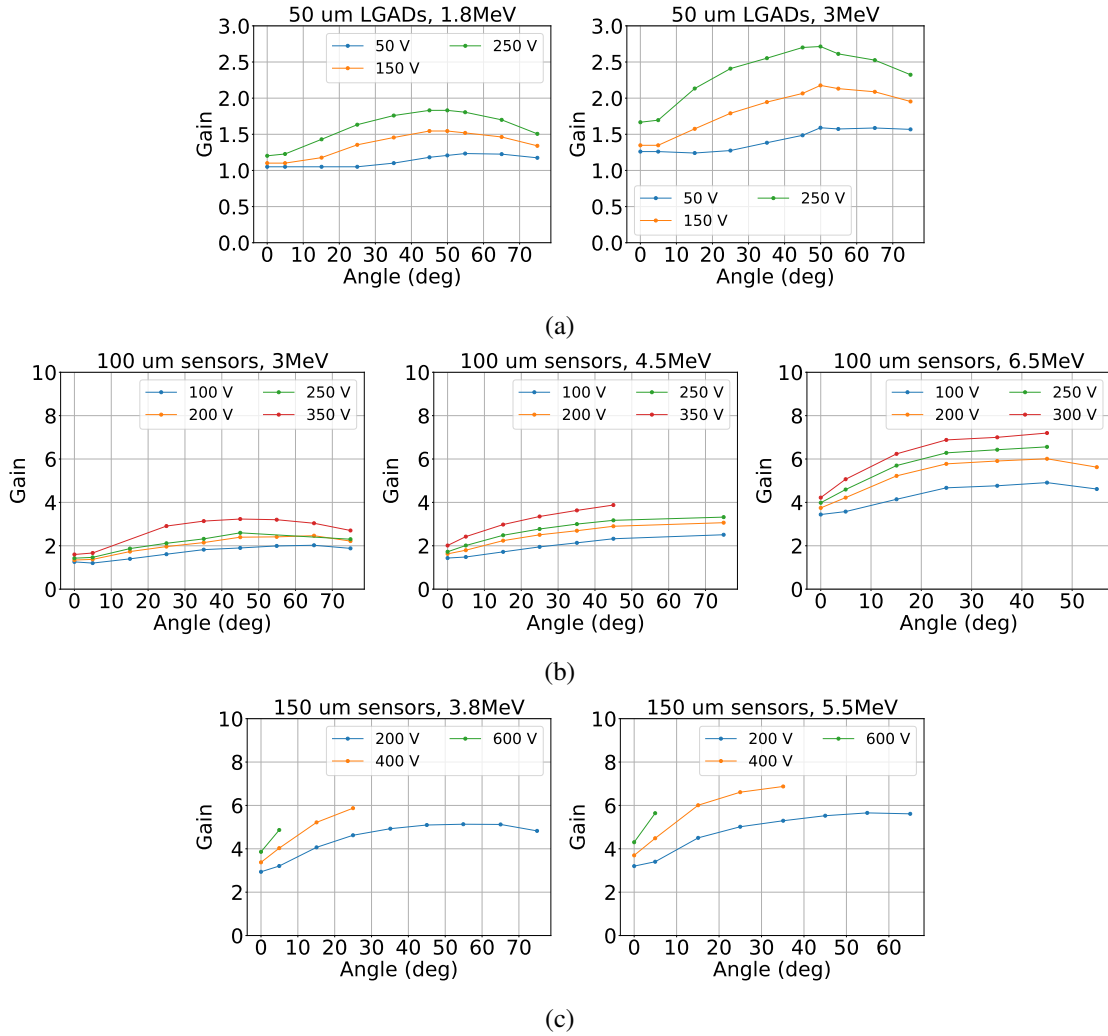


Figure 2: Gain as a function of angle for different bias voltages for the three FBK LGADs at different energies. Particular runs were not included due to saturation in either the amplifier or digitizer for larger gains.

behavior is the difference in doping profile between HPK and FBK sensors; the latter have a very shallow gain layer². A shallow gain layer has a very compact high-field region, which leads to a higher charge density after the multiplication starts, causing a higher suppression effect.

A series of detectors fabricated for ATLAS and CMS timing layers from HPK and FBK with different doping concentrations and profiles will be considered for the next data-taking campaign. This focused study will probe the gain suppression for different gain layer configurations; the final goal is to fabricate a device that is as linear as possible on a large range of deposited energies for the PIONEER experiment.

²Detailed doping profiles are protected information of HPK and FBK, so they cannot be disclosed

7 Acknowledgments

This work was supported by the United States Department of Energy grants DE-SC0010107, DE-FG02-04ER41286, and DE-FG02-97ER41020. We thank the CENPA Technical and Accelerator staff for their assistance in this measurement.

References

- [1] G. Pellegrini et al., *Technology developments and first measurements of Low Gain Avalanche Detectors (LGAD) for high energy physics applications*, *Nucl. Instrum. Meth.* **A765** (2014) 12 – 16.
- [2] Y. Zhao et al., *Comparison of 35 and 50 μm thin HPK UFSD after neutron irradiation up to $6 \cdot 10^{15}$ neq/cm²*, *Nucl. Instrum. Meth. A* **924** (2019) 387–393, [[1803.02690](#)].
- [3] ATLAS collaboration, HGTD, *Technical Design Report: A High-Granularity Timing Detector for the ATLAS Phase-II Upgrade*, Tech. Rep. CERN-LHCC-2020-007. ATLAS-TDR-031, CERN, Geneva, Jun, 2020.
- [4] CMS collaboration, *A MIP Timing Detector for the CMS Phase-2 Upgrade*, Tech. Rep. CERN-LHCC-2019-003. CMS-TDR-020, CERN, Geneva, Mar, 2019.
- [5] Electron-Ion collider, “<https://www.bnl.gov/eic/>.”
- [6] PIONEER collaboration, S. M. Mazza, *An LGAD-Based Full Active Target for the PIONEER Experiment*, *Instruments* **5** (2021) 40, [[2111.05375](#)].
- [7] S. Braun et al., *Gain suppression study on LGADs at the CENPA tandem accelerator*, *Nucl. Instrum. Meth. A* **1064** (2024) 169395, [[2405.02550](#)].
- [8] M. C. J.-R. et al., *Study of ionization charge density-induced gain suppression in LGADs*, *Sensors* **22** (2022) .
- [9] E. Currás, M. Fernández and M. Moll, *Gain reduction mechanism observed in Low Gain Avalanche Diodes*, *Nucl. Instrum. Meth. A* **1031** (May, 2022) 166530.
- [10] D. S. et al., *Status of and operating experience with the university of washington superconducting booster linac*, *Nucl. Instrum. Meth A* 287, 247 (1990) .
- [11] R. P. et al., *Effect of deep gain layer and carbon infusion on LGAD radiation hardness*, *Journal of Instrumentation* **15** (2020) P10003.
- [12] D. Breton, C. Cheikali, E. Delagnes, J. Maalmi, P. Rusquart and P. Vallerand, *Fast electronics for particle Time-Of-Flight measurement, with focus on the SAMPIC ASIC*, *Nuovo Cim. C* **43** (2020) 7.
- [13] S. M. Mazza et al., *Synchrotron light source X-ray detection with Low-Gain Avalanche Diodes*, *Journal of Instrumentation* **18** (2023) P10006, [[2306.15798](#)].
- [14] A. Molnar et al., *Synchrotron light source focused X-ray detection with LGADs, AC-LGADs and TI-LGADs*, [2504.18638](#).